Proc. 13th Int. Conf. on Nucleus-Nucleus Collisions
JPS Conf. Proc. **32**, 010066 (2020)
https://doi.org/10.7566/JPSCP.32.010066

Nuclear Symmetry Energy and the Breaking of the Isospin Symmetry: How Do They Reconcile with Each Other ?

Hiroyuki Sagawa[1,2], Xavier Roca-Maza[3,4] and Gianluca Colò[3,4]

[1]*RIKEN Nishina Center, Wako, Saitama 351-0198, Japan*
[2]*Center for Mathematics and Physics, University of Aizu, Aizu-Wakamatsu, Fukushima 965-8580, Japan*
[3]*Dipartimento di Fisica "Aldo Pontremoli", Università degli Studi di Milano, Via Celoria 16, 20133 Milano (Italy)*
[4]*INFN, Sezione di Milano, Via Celoria 16, 20133 Milano (Italy)*

E-mail: sagawa@ribf.riken.jp

(Received July 26, 2019)

A fully self-consistent HF+RPA model is applied to study the IAS in ^{208}Pb. We perform state-of-the-art calculations of all possible contributions to the excitation energy of IAS in ^{208}Pb, including the isospin breaking contributions from the charge symmetry breaking and the charge independence breaking intractions in the Skyrme-type EDF without compromising other properties of the EDF. The calculated results give a fine agreement with the experimental excitation energy of IAS in ^{208}Pb reconciling realistic symmetry energy parameters and the neutron skin. The same EDF reproduces also IAS energies of Sn isotopes well.

KEYWORDS: Isobaric Analog States, Neutron Skin, Symmetry Energy, Charge Symmetry and Charge Independent forces.

1. Introduction

The density dependence of symmetry energy is still not understood well enough. A deeper understanding is highly needed, because an accurate characterization of the symmetry energy entails profound consequences for the study of neutron distributions in nuclei along the entire nuclear chart, as well of other properties of neutron-rich nuclei [1]. The symmetry energy is also of paramount importance for understanding the properties of compact objects like neutron stars; it directly affects the determination of the radius of a low-mass neutron star [2]. Neutron star physics have received a new strong boost very recently, as the LIGO-Virgo collaboration announced the first detection of gravitational waves from neutron star merger [3].

Defining δ as the local neutron-proton asymmetry, $\delta \equiv (\rho_n - \rho_p)/\rho$, the energy per particle in matter having arbitrary neutron-proton imbalance is a function $\frac{E}{A}(\rho, \delta)$. Such function can be expanded in even powers of δ owing to isospin symmetry (the Coulomb force has to be taken out when dealing with a uniform system). By retaining only the quadratic term we can write

$$e(\rho, \delta) \equiv \frac{E}{A}(\rho, \delta) = \frac{E}{A}(\rho, \delta = 0) + S(\rho)\delta^2. \tag{1}$$

This equation defines the symmetry energy $S(\rho)$, that is, the difference between the energy per particle E/A in neutron and symmetric matter. Eq. (1) clearly explains why an accurate knowledge of the symmetry energy is mandatory in order to establish a link between the physics of finite nuclei and the neutron star physics.

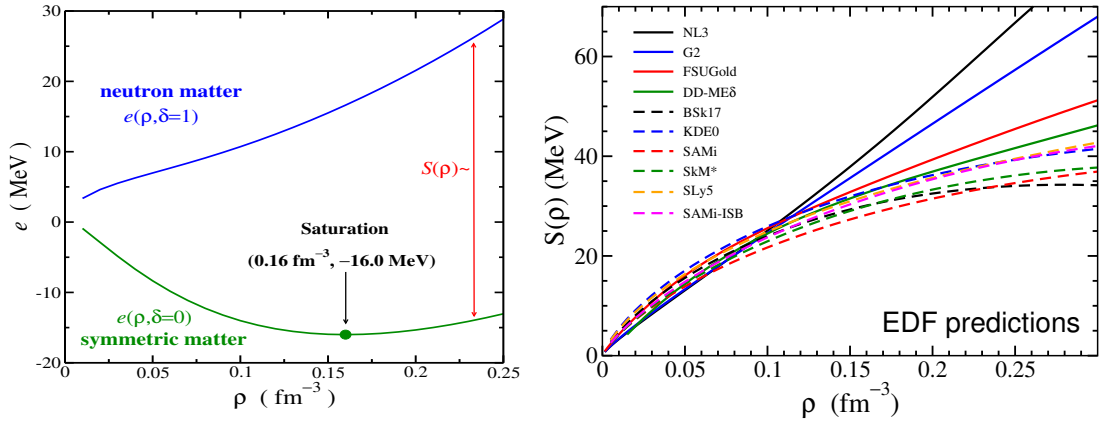

Fig. 1. (left) Nuclear equation of state (EoS) of nuclear matter and neutron matter. (right) Symmetry energy with various energy density functionals (EDFs). Relativistic models are shown by full lines, while Skyrme models are shown by dashed lines.

The symmetry energy can be expanded by in a power series of $(\rho - \rho_0)$ as

$$S(\rho) = J + L\frac{\rho - \rho_0}{3\rho_0} + \frac{1}{2}K_{sym}(\frac{\rho - \rho_0}{3\rho_0})^2 + ..., \tag{2}$$

where ρ_0 is the saturation density and

$$J \equiv S(\rho_0), \quad L \equiv 3\rho_0\, S'(\rho_0), \quad K_{\rm sym} \equiv 9\rho_0^2\, S''(\rho_0), \tag{3}$$

on which much attention has been focused. While $K_{\rm sym}$ is basically not known, the error on L, referred to as the "slope parameter", is believed to be still significantly larger than the error on J: a range between ≈ 40-75 MeV or between ≈30-90 MeV are mentioned in Refs. [2, 4–7].

Nuclear matter and neutron matter equation of state (EoS) are shown in the left panel of Fig. 1. The symmetry energy defined by the difference between neutron and nuclear matter EoS is shown in the right panel of Fig. 1. As one can see, there are large variety of values and density dependences for the symmetry energy among different theoretical models, especially between relativistic and Skyrme models. The difficulties in determining the symmetry energy behavior are associated with our still incomplete understanding of the strong interaction in the low-energy regime that is important for nuclei. The isobaric analog state (IAS) is one of the well-established properties of nuclei that is measured accurately, and it is dominantly sensitive to the isospin symmetry breaking (ISB) in the nuclear medium due to Coulomb interaction [8] and, to a lesser extent, the other effects that we will discuss below. If there is an inconsistency between the properties of the symmetry energy and our knowledge of the IAS and ISB forces, it is a serious issue. As discussed often, the neutron skin is strongly correlated with the density dependence of the symmetry energy [9]. Therefore, we cannot accept that the values of the neutron skin do not match our understanding of the isospin symmetry, which is one of the basic symmetries of nature, and its breaking.

2. Self-consistent HF+RPA calculations

The calculations of IAS states are done within the framework of the Skyrme Hartree-Fock (HF) plus charge-exchange Random Phase Approximation (RPA) [13, 14]. We adopt the standard form of Skyrme interactions with the notations of Ref. [15]. Our charge-exchange RPA had been first introduced and illustrated in Ref. [13] and further improved in Ref. [14], to which we refer the reader for details. Some details that are common between charge-exchange and normal RPA can be found

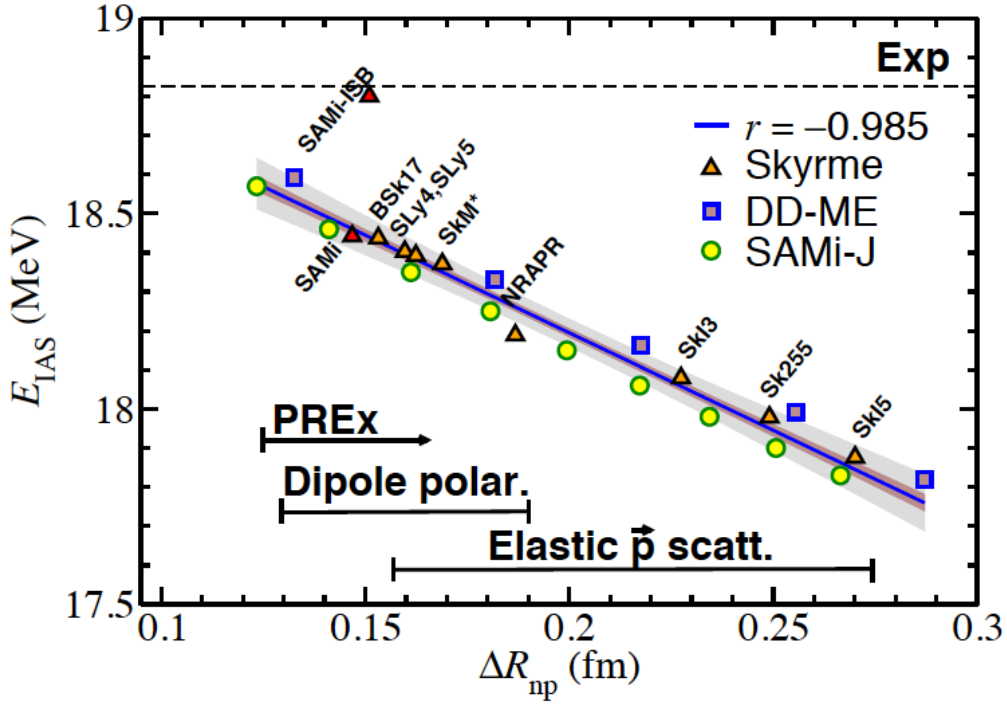

Fig. 2. Energy of the IAS as a function of the neutron skin of ^{208}Pb ΔR_{np} with various EDFs. The arrows indicate the experimental results; PREx is obtained from the polarized electron parity violation experiment [10], Dipole polarizability is the value obtained from the measurement of giant dipole resonances [11], and elastic p scattering is the data obtained from the polarized proton scattering cross section analysis [12]. The lower limit of PREx data is shown in the figure since the central value ΔR_{np}=0.302 is outside of the maximum value of this plot.

in Ref. [16], where HF-RPA for non charge-exchange modes is fully discussed. Within the Skyrme functionals, SAMi has been shown to be particularly accurate in the description of charge-exchange resonances such as the Gamow-Teller resonance. Starting from the prototype SAMi functional [17], a systematically varied family was generated, by keeping a similar quality of the original fit and varying the values of J and L. In addition, a family based on the systematic variation of J and L with respect to a relativistic mean field (RMF) model with density-dependent meson-nucleon vertices (DD-ME) [18] was also introduced. These functionals provide the values of the neutron skin through the Hartree-Fock (HF) or Hartree solution for the ground-state; in addition, they provide, self-consistently, the IAS energy via the charge-exchange random phase approximation (RPA).

The results for the IAS energy, E_{IAS}, as a function of ΔR_{np} are plotted in Fig. 2. The results associated with other Skyrme interactions are also plotted. We found a serious discrepancy of $\approx$ 0.5-1 MeV between the calculated and experimental E_{IAS} for all EDFs in Fig. 2 (SAMi-ISB should be excluded at this stage as we will discuss below). To solve the puzzle, we reconsidered all possible contributions to the IAS energy that have not been considered with sufficient care in self-consistent calculations so far. Then, we proposed a new parametrization SAMi-ISB for Skyrme-like EDF, which reconciles standard nuclear properties (saturation density, binding energy, and charge radii of finite nuclei) with both our current understanding of the density behavior of the symmetry energy and the reproduction of the IAS energy of ^{208}Pb as well as those of Sn isotopes [19, 20].

The fitting protocol of SAMi-ISB is based on a χ^2 minimization and it is identical to that re-

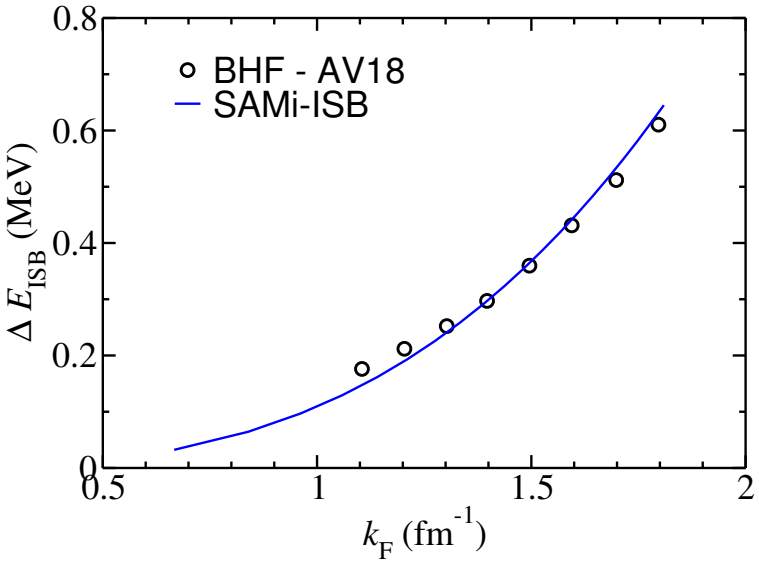

Fig. 3. ISB contributions to the symmetric matter equation of state as predicted by the BHF calculations based on AV18 potential (black circles). The solid line is the optimal fit of this quantity.

ported in Ref. [21] in the case of the SAMi interaction, except for the inclusion in the χ^2 of: (i) the experimental value of the excitation energy of the Isobaric Analog State in ^{208}Pb [15] (E_{IAS}) with an adopted error of E_{IAS} = 30 keV in agreement with the very accurate determination of this quantity; and (ii) the isospin symmetry breaking (ISB) contributions to the symmetric nuclear matter equation of state (EoS) as calculated by the benchmark Brueckner-Hartree-Fock (BHF) calculations based on AV18 [22] reported in reference [23]. We have fitted 9 data points (as shown in Fig. 3) and the adopted error for each of them has been taken to be 10 keV.

SAMi-ISB includes CSB and CIB terms. In fact, following Ref. [24] [cf. Eqs.(18-21)], we have written then in a simple Skyrme-like form as follows,

$$V_{\rm CSB}(\vec{r}_1,\vec{r}_2) = \frac{1}{4}\left[\tau_z(1)+\tau_z(2)\right] s_0(1+y_0P_\sigma)\delta(\vec{r}_1-\vec{r}_2), \tag{4}$$

and

$$V_{\rm CIB}(\vec{r}_1,\vec{r}_2) = \frac{1}{2}\tau_z(1)\tau_z(2)u_0(1+z_0P_\sigma)\delta(\vec{r}_1-\vec{r}_2). \tag{5}$$

Table I. Effect of the different contributions mentioned in the text on the IAS energy in ^{208}Pb. These corrections are basically model-independent except the ISB one. The precise values of contributions from the interaction ISB (including both CSB and CIB) are introduced in Ref. [19]. The calculation of HF+RPA in the first line is performed by the Slater approximation for the Coulomb exchange.

	$E_{\rm IAS}$ [MeV]	Correction [keV]	$E_{\rm IAS}$ (Exp) [MeV]
HF+RPA	18.31		
+Exact Coulomb exchange	18.41	+100	
+n/p mass difference	18.44	+30	
+Electromagnetic spin-orbit	18.45	+10	
+Finite size effects	18.40	-50	
+Vacuum polarization ($V_{\rm ch}$)	18.53	+130	
+Isospin symmetry breaking	18.80	+270	18.826 ± 0.010

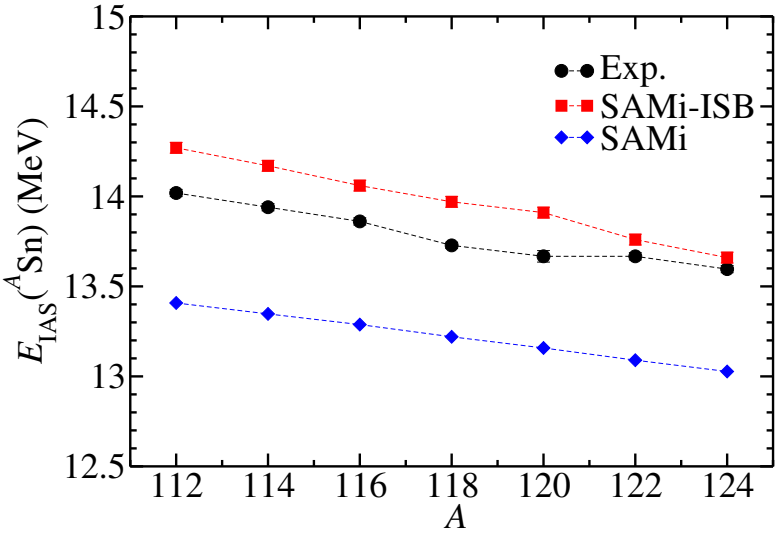

Fig. 4. E_{IAS} for Sn isotopes as predicted by SAMi and SAMi-ISB, compared to experimental data.

Here, P_σ is the usual spin exchange operator. The simplicity consists in assuming that the CSB and CIB forces are just a delta-function depending on s_0 and u_0 (with $y_0 = -1$ and $z_0 = -1$); the momentum-dependent terms have not been considered, under the rationale that the information that we have at our disposal is not sufficient to pin down the values of all parameters of a general interaction with several partial waves (see, however, Ref. [25]). The EDF terms produced by CSB and CIB interactions are given by

$$\langle V_{\rm CSB}\rangle = \int d\mathbf{r}\frac{1}{8}s_0(1-y_0)(\rho_n^2-\rho_p^2), \tag{6}$$

and

$$\langle V_{\rm CIB}\rangle = \int d\mathbf{r}\frac{1}{8}\left[u_0(1-z_0)(\rho_n^2+\rho_p^2)-u_0(2+z_0)\rho_n\rho_p\right] \tag{7}$$

(more details can be found in Ref. [26]). In Fig. 3, the CIB part of Bruckner HF with AV18 interaction is plotted and compared with SAMi-ISB results. It is remarkable that the density dependence (k_F dependence) of CIB from Brueckner HF agrees well with that of the Skyrme EDF, having the ρ-dependence $V_{\rm CIB}/\rho \propto u_0\rho$ extracted from Eq. (7) in nuclear matter.

Various contributions to E_{IAS} are tabulated in Table 1. The first line denoted by "no corrections" is the RPA result with Slater approximation for the Coulomb exchange term. The exact Coulomb calculation provides a shift of 100 keV upwards. Four contributions, the n-p mass difference, electromagnetic spin-orbit correction, effect of finite proton and neutron sizes, and effect of vacuum polarization produce an overall upward shift of the IAS energy which is about 120 keV. These contributions, however, are too small in order to let the line intersect the experimental value for the IAS energy at a point that corresponds to a realistic range of $\Delta R_{\rm np}$ indicated by the horizontal bars in Fig. 2. In Table I we can see that the overall shift, by adding all the small effects, amounts to $\approx$ 220 keV. The CSB and CIB contributions make this shift double and give a realistic range of $\Delta R_{\rm np}$ as seen from the symbol marked SAMi-ISB in Fig. 2.

The E_{IAS} for the case of some measured Sn isotopes, as predicted by SAMi and SAMi-ISB, are shown in Fig. 4. As expected, the results have been remarkably improved with respect to the results

of the SAMi interaction. The IAS energies calculated with SAMi differ from the experimental values by about 600 keV, while this discrepancy is reduced to 50-200 keV by using SAMi-ISB. In these calculations pairing correlations have been neglected since we have checked that their effects are of the order of the statistical error around tens of keV as reported in Ref. [19]. We extend our predictions also to ^{48}Ca and ^{90}Zr. In these cases, the results are also improved with respect to SAMi.

3. Conclusions

In conclusion, SAMi-ISB is a new parameterization of a Skyrme-like energy density functional (EDF) that reconciles standard nuclear properties (saturation density, binding energy and charge radii of finite nuclei) with both our current understanding of the density behavior of the symmetry energy and the reproduction of the IAS energy of ^{208}Pb as well as those of Sn isotopes. We have self-consistently included for the first time within the HF+RPA framework all known contributions that break the isospin symmetry. All of these contributions are calculated in a model-independent way, except the CSB-CIB contribution. We have fixed only two free parameters in the CSB-CIB terms, and we have shown that this allows reproducing at the same time BHF calculations based on AV18, and the IAS energies of heavy nuclei such as ^{208}Pb and Sn isotopes without compromising the other properties of nuclear matter and finite nuclei.

References

[1] Bao-An Li *et al*., Eur. Phys. J. A50, 9 (2014).
[2] C. J. Horowitz *et al*., J. Phys. G41, 093001 (2014).
[3] B. P. Abbott, R. Abbott, T. D. Abbott, F. Acernese, K. Ackley, C. Adams, T. Adams, P. Addesso, and R. X. Adhikari (LIGO Scientific Collaboration and Virgo Collaboration), Phys. Rev. Lett. 119, 161101 (2017).
[4] J. M. Lattimer and Y. Lim, The Astrophysical Journal 771, 51 (2013).
[5] B.-A. Li and X. Han, Phys. Lett. B 727, 276 (2013).
[6] M. Oertel, M. Hempel, T. Klähn, and S. Typel, Rev. Mod. Phys. 89, 015007 (2017).
[7] X. Roca-Maza and N. Paar, Progress in Particle and Nuclear Physics 101, 96 (2018).
[8] N. Auerbach *et al*., Phys. Rev. Lett. 23, 484 (1969).
[9] X. Roca-Maza, M. Centelles, X. Viñas, and M. Warda, Phys. Rev. Lett. 106, 252501 (2001).
[10] C. J. Horowitz et al., Phys. Rev. C85, 032501 (2012).
[11] A. Tamii et al., Phys. Rev. Lett. 107, 062502 (2011).
[12] J. Zenihiro et al., Phys. Rev. C82, 044611 (2010).
[13] G. Colò, N. Van Giai, P. F. Bortignon, and R. A. Broglia, Phys. Rev. C 50, 1496 (1994).
[14] X. Roca-Maza, L.-G. Cao, G. Colò, and H. Sagawa, Phys. Rev. C 94, 044313 (2016).
[15] E. Chabanat, P. Bonche, P. Haensel, J. Meyer, and R. Schaeffer, Nucl. Phys. A 627, 710 (1997).
[16] G. Colò, L. Cao, N. V. Giai, and L. Capelli, Comp. Phys. Comm. 184, 142 (2013).
[17] X. Roca-Maza, G. Colò, and H. Sagawa, Phys. Rev. C 86, 031306 (2012).
[18] D. Vretenar, T. Niksic, and P. Ring, Phys. Rev. C 68, 024310 (2003).
[19] X. Roca-Maza, G. Colò, and H. Sagawa, Phys. Rev. Lett. 120, 202501 (2018).
[20] X. Roca-Maza, G. Colò, and H. Sagawa, EPJ Web of Conferences 194, 01002 (2018).
[21] X. Roca-Maza, G. Colò, and H. Sagawa, Phys. Rev. C 86, 031306 (2012).
[22] R. B. Wiringa, V. G. J. Stoks, and R. Schiavilla, Phys. Rev. C 51, 38 (1995).
[23] H. Muther, A. Polls, and R. Machleidt, Physics Letters B 445, 259 (1999).
[24] H. Sagawa, N. V. Giai, and T. Suzuki, Physics Letters B 353, 7 (1995).
[25] P. Baczyk, J.Dobaczewski, M.Konieczka, W.Satula, T.Nakatsukasa, and K.Sato, Phys. Lett. B778, 178 (2018).
[26] H. Sagawa, G. Colò, X. Roca-Maza, Y.F. Niu, Eur. Phys. J A (submitted).